THEMIS SIGNAL ANALYSIS STATISTICS RESEARCH PROGRAM

AN APPROXIMATE FOURIER INTEGRAL TRANSFORM METHOD FOR ANALYSIS OF WAVE PROPAGATION SIGNALS

by

Hal Watson, Jr.

Technical Report No. 73
Department of Statistics THEMIS Contract

July 13, 1970

Research sponsored by the Office of Naval Research
Contract N00014-68-A-0515
Project NR 042-260

DEPARTMENT OF STATISTICS
Southern Methodist University

LIST OF SYMBOLS

SYMBOL	
t	Time (sec)
ω	Circular frequency (sec^{-1})
$f(t)$	Time function
T	Time interval (sec)
N	Positive integer
n	Summation integer index
Δt	Time increment (sec)
Δf	Frequency increment (cps)
i	$\sqrt{-1}$
$\Delta\omega$	Circular frequency increment (sec^{-1})
k	Integer index
$\overset{*}{f}(t)$	Piecewise linear approximating time function
$\bar{f}(\omega)$	Integral Fourier transform of $f(t)$
$\overset{*}{\bar{f}}(\omega)$	Fourier integral transform of approximating function $\overset{*}{f}(t)$
f_n	Value of $f(t)$ at $t = t_n$
$\overset{*}{\bar{f}}(\omega)$	Piecewise linear approximating frequency function
$\bar{f}_k$	Value of $\bar{f}(\omega)$ at $\omega = \omega_k$
η	Integer index
$\hat{f}(t)$	Inverse Fourier integral transform of $\overset{*}{\bar{f}}(\omega)$
e^x or $\exp(x)$	Complex exponential function
$\psi(x,t)$	Wave function
$\bar{\psi}(x,\omega)$	Fourier transform of wave function
$\lambda(\omega)$	Complex wave number
$\alpha(\omega)$	Attenuation coefficient (in^{-1})
$C(\omega)$	Phase velocity (in/sec)
σ	Stress (lb/in^2)
V	Particle velocity (in/sec)

SYMBOL	
ρ	Mass density ($lb\text{-}sec^2/in$)
$\overset{*}{C}$	Complex phase velocity (in/sec)
L	Distance between two data stations (in.)
T_p	First arrival time of wave at second data station (sec.)
Re{ }	Real part of a complex quantity
Im{ }	Imaginary part of a complex quantity

INTRODUCTION

The wave equation with a complex phase velocity in one spatial dimension has been shown to govern the motion of plane waves in dispersive and dissipative media such as (a) water containing a large concentration of air bubble scatters[1] or, (b) viscoelastic polymers[2], to name only two. In studying wave motion in such media, two types of problems are often encountered, (1) determination of the complex phase velocity and attenuation coefficient from experimental data obtained at two spatial locations during the passage of the wave and, (2) prediction of the response of the medium at some spatial location given the value of the complex phase velocity and attenuation of the medium and the wave function at some other spatial location. In the case of the stress wave propagating along a viscoelastic bar, the first problem corresponds to determining the phase velocity and attenuation parameter given the particle velocity-time or strain-time data at two points along the bar. The second case corresponds to predicting the stress, strain, or particle velocity at some downstream point along the bar given the phase velocity and attentuation parameter and the stress-time, strain-time, or particle velocity-time data at some upstream point.

In both problems mentioned above, the solution often involves taking either the integral Fourier transform of the wave function, as in Problem (1) above, or the inverse integral Fourier transform of some response function, as in Problem (2) above. Usually, the Fourier transforms are obtained numerically because the wave function-time data is such a complex function of time that analytic expressions of the transforms are extremely difficult to obtain. Recently Magrab[3] has shown that even approximate numerical methods of obtaining the inverse Fourier transform in obtaining the response of a viscoelastic bar are difficult and tedious to apply.

In the discussion that follows, an analytical-numerical method of obtaining integral Fourier and inverse integral Fourier transforms is discussed. The technique has been used to obtain the approximate transforms of functions, the real transforms of which are known.

THE ANALYTICAL-NUMERICAL METHOD

We are given the function f(t) (Fig. 1) which is real for $0 \leq t \leq T$ and zero for t outside the interval. The Fourier integral transform for such a function is

$$(1) \quad \bar{f}(\omega) = \int_0^T f(t)e^{i\omega t}dt$$

the inverse transform of which is

$$(2) \quad f(t) = \frac{1}{\pi}\int_0^\infty \bar{f}(\omega)e^{i\omega t}d\omega \quad \text{for } f(t) \text{ real.}$$

The usual numerical method of evaluating (1) is to approximate the function f(t) with a time series and the integral with a finite summation; thereby forming the discrete Fourier transform.

$$(3) \quad \bar{f}(\omega) \simeq \sum_{n=0}^{N-1} f(n\Delta t)\exp(i\omega n\Delta t)\Delta t$$

in which the interval $0 \leq t \leq T$ is divided into N-1 equal time intervals in which

$$(4) \quad \Delta t = \frac{T}{(N-1)}$$

and the summation is performed at certain discrete values of ω at which $\bar{f}(\omega)$ is simply related to the integral transform of f(t)[4]. For large N this method requires a great amount of computer time and has been replaced in recent years by the so-called "Fast Fourier Transform"(FFT) made possible by the Cooley-Tukey[5] algorithm which takes advantage of certain symmetric properties of the transform and periodicity relations in computing complex exponentials but still uses the form of (3) above to generate transforms. The FFT method reduces the number of operations from order N^2 to order N log N*; thereby effecting a great saving in computer time for large N.

*for $\omega = k\Delta\omega$, $k = 0,1,2...N$.

The method described below should require more computer time than the FFT method for the same number of data points N since the method below requires several additional computations at each value of ω. However, it will become obvious that the number of data points required to obtain an accurate numerical approximation of the transform is less for the method below than for any method which uses (3) as its basis and should therefore be faster than even the FFT method provided the same efficient use of symmetry and periodicity relationships are used as in the FFT method.

INTEGRAL TRANSFORM

Given the function $f(t)$, $0 \leq t \leq T$ (see Fig. 1), we form a piecewise linear approximation of the function between abscissa points t_n and t_{n+1} corresponding to ordinates f_n and f_{n+1} respectively. An approximate description of $f(t)$ between t_n and t_{n+1} is then

$$(5)\quad \Delta_n(t): \begin{cases} = 0\ , & t < t_n \\ = f_n + \dfrac{f_{n+1} - f_n}{t_{n+1} - t_n}\,(t - t_n), & t_n \leq t \leq t_{n+1} \\ = 0\ , & t > t_{n+1} \end{cases}$$

which is shown in Fig. 2. An approximation to $f(t)$ over the entire interval $0 \leq t \leq T$ can then be expressed as a series of such functions or

$$(6)\quad \overset{*}{f}(t) = \sum_{n=0}^{N-1} \Delta_n(t) \simeq f(t)$$

in which N is the number of intervals of connected linear approximations to $f(t)$. The intervals are not necessarily equal. The approximate Fourier transform of $f(t)$ is then

$$(7)\quad \overset{*}{\bar{f}}(\omega) = \sum_{n=0}^{N-1} \bar{\Delta}_n(\omega) \simeq \bar{f}(\omega) \qquad \text{where}$$

$$(8)\quad \bar{\Delta}_n(\omega) = \int_{t_n}^{t_{n+1}} \Delta_n(t)\, e^{-i\omega t}\, dt.$$

Substituting (5) into (8) we have:

$$(9)\quad \bar{\Delta}_n(\omega) = \int_{t_n}^{t_{n+1}} \left\{ f_n + \frac{f_{n+1} - f_n}{t_{n+1} - t_n} (t - t_n) \right\} e^{-i\omega t} dt \quad ,$$

which after integrating by parts is

$$(10)\quad \bar{\Delta}_n(\omega) = \left\{ \left[\frac{f_n - f_{n+1}}{\omega^2 (t_{n+1} - t_n)} \right] \left[1 - e^{-i\omega(t_{n+1} - t_n)} \right] + \frac{f_n - f_{n+1} e^{-i\omega(t_{n+1} - t_n)}}{i\omega} \right\} e^{-i\omega t_n}$$

for $\omega > 0$. For $\omega = 0$ we have from (9)

$$(11)\quad \bar{\Delta}_n(0) = f_n(t_{n+1} - t_n) + \frac{1}{2}(f_{n+1} - f_n)(t_{n+1} - t_n)$$

$$= \frac{1}{2}(f_{n+1} + f_n)(t_{n+1} - t_n)$$

Equations (10) and (11) can be substituted into (7) to obtain:

$$(12)\quad \bar{f}(0) \simeq \bar{\bar{f}}(0) = \sum_{n=0}^{N-1} \left\{ f_n(t_{n+1} - t_n) + \frac{1}{2}(f_{n+1} - f_n)(t_{n+1} - t_n) \right\}$$

$$(13)\quad \underset{\omega>0}{\bar{f}(\omega)} \simeq \underset{\omega>0}{\bar{\bar{f}}(\omega)} = \sum_{n=0}^{N-1} \left\{ \left[\frac{f_n - f_{n+1}}{\omega^2 (t_{n+1} - t_n)} \right] \left[1 - \exp(-i\omega(t_{n+1} - t_n)) \right] + \frac{f_n - f_{n+1} \left[\exp(-i\omega(t_{n+1} - t_n)) \right]}{i\omega} \right\} \exp(-i\omega t_n) \quad ,$$

which is the analytical integral Fourier transform of the piecewise linear approximation to f(t) composed of N-1 linear sigments connecting N data points.

Equations (12) and (13) are easily programmed for solution on a digital computer (see Appendix) especially one having the complex exponential as a

library function. Computation of $\bar{\bar{f}}^*(\omega)$ involves executing only two "DO" loops after the N values of each of f_n and t_n are read into storage; one "DO" loop index determines the value of ω, the other, n.

An interesting comparison between this technique and the discrete Fourier Transform described by Eqn. (3) can be made by allowing the approximating function $\bar{\bar{f}}^*(t)$ to be composed of equally spaced flat-topped segments as seen in Fig. 4. This can be effected by permitting $f_{n+1} = f_n$ in Eqn. (5) and (9) and the result of integrating (9) is

$$(14) \quad \bar{\Delta}_n(\omega) = f_n \frac{\sin(\omega\Delta t)}{(\omega\Delta t)} \; e^{-i\omega t_n} \; \Delta t$$

where $\Delta t = t_{n+1} - t_n$. Substituting (14) into (7) we obtain

$$(15) \quad \bar{f}(\omega) \simeq \bar{\bar{f}}^* = \left(\sum_{n=0}^{N-1} f_n \exp[-i\omega n\Delta t]\Delta t \right) \frac{\sin \omega\Delta t}{\omega\Delta t}$$

and we see in Eqn. (15) that the analytical Fourier integral transform of the approximating function made up of flat-topped functions (Fig. 4,5) is the same as the finite difference approximation to the integral transform (discrete transform) of f(t), as shown in Eqn. (3), except for the multiplying factor:

$$(16) \quad \frac{\sin(\omega\Delta t)}{(\omega\Delta t)} = \frac{\sin(\omega T/N)}{(\omega T/N)}$$

which approaches unity as $\omega T/N \to 0$. For sufficiently large N, then, the discrete transform given by Eqn. (3) is very nearly equal to the analytic transform of $\bar{\bar{f}}^*(t)$ described by the flat-topped functions in Fig. 4.

NUMERICAL RESULTS

Transforms of a half sine pulse and a triangular pulse were computed using Eqn. (3) and (15). Very good agreement was achieved between the two methods and the known analytic transforms for $\omega T/N < 0.1$. For $\omega T/N > 0.1$ Eqn. (15) yielded the better result though neither (3) nor (15) compared favorably with the known transform.

The Fourier integral transform of the triangular function shown in Fig. 6 was calculated on a digital computer using Eqn. (12) and Eqn. (13) for $T = 10^{-4}$ sec. and $N = 100$. The values computed using the analytical-numerical method were found to be the same for either $N = 3$ data points selected at $-T$, 0, and $+T$ or for $N = 100$, and the values were found to agree with the known analytic values of the integral transform of the function to six significant digits out to $\omega T = 5$ (five zeros of the transform), where the calculations were terminated (see Program One output, columns two and four). Computed values using the discrete-finite difference method of Eqn. (3) for $N = 100$ agreed with the exact values to three significant digits over the interval $0 \leq \omega T \leq 5$ (see Program One output columns four and six). This test case is perhaps the most dramatic example one could use to show superiority of the analytical-numerical method since, because $f(t)$ in Fig. 6 is comprised of linear segments only, Eqn. (15) is exact. Less dramatic superiority was indicated in computing transforms of nonlinear functions. This is demonstrated in the next section below.

INVERSE INTEGRAL TRANSFORM

An approximate inverse Fourier integral transform of a function $\bar{f}(\omega)$ can be obtained in the same manner as the approximate transform was obtained for the function $f(t)$ in the previous section.

Given the function $\bar{f}(\omega)$ (see Fig. 7) the inverse integral transform of the real function $f(t)$ is, after taking advantage of the symmetry of the transform,

$$(17) \quad f(t) = \frac{1}{\pi} \int_0^{\infty} \bar{f}(\omega)\, e^{i\omega t}\, d\omega$$

As in the previous section for $f(t)$, we form an approximating function $\overset{*}{\bar{f}}(\omega)$, which approximates $\bar{f}(\omega)$ by means of piecewise linear segments at regular or irregular intervals, as shown in Fig. 8. Then

$$(18) \quad f(\omega) \simeq \overset{*}{\bar{f}}(\omega) = \sum_{k=0}^{M} \bar{\delta}_k(\omega)$$

in which

$$(19)\quad \bar{\delta}_k(\omega) = \begin{cases} 0 \quad , \ \omega < \omega_k \\ \bar{f}_k + \dfrac{\bar{f}_{k+1} - \bar{f}_k}{\omega_{k+1} - \omega_k}\ \omega \quad , \ \omega_k \le \omega \le \omega_{k+1} \\ 0 \ , \ \omega_{k+1} < \omega \end{cases}$$

which is described in Fig. 9. The inverse integral of $\bar{f}(\omega)$ is then approximated by

$$(20)\quad f(t) \simeq \hat{f}(t) = \sum_{k=0}^{M} \delta_k(t)$$

where

$$\delta_k(t) = \frac{1}{\pi} \int_{\omega_k}^{\omega_{k+1}} \bar{\delta}_k(\omega) e^{i\omega t}\, d\omega$$

$$(21)\quad = \frac{1}{\pi} \int_{\omega_k}^{\omega_{k+1}} \left\{ \bar{f}_k + \frac{\bar{f}_{k+1} - \bar{f}_k}{\omega_{k+1} - \omega_k}\ \omega \right\} e^{i\omega t}\, d\omega$$

After integrating Eqn. (21) by parts, we obtain

$$(22)\quad \delta_k(t) = \frac{1}{\pi} \left\{ \frac{1}{2}(\bar{f}_{k+1} + \bar{f}_k)(\omega_{k+1} - \omega_k) \right\} \qquad \text{for } t = 0$$

$$= \frac{1}{\pi} \left\{ \left[\frac{\bar{f}_k - \bar{f}_{k+1}}{(\omega_{k+1} - \omega_k)} \right] \left[1 - e^{i(\omega_{k+1} - \omega_k)t} \right] \right.$$

$$\left. - \left[\frac{\bar{f}_k - \bar{f}_{k+1} e^{i(\omega_{k+1} - \omega_k)t}}{it} \right] \right\} e^{i\omega_k t}$$

for $t > 0$

Equation (22) can be substituted into Eqn. (20) which can be used to compute the analytical transform $\hat{f}(t)$ of the approximating function made up

of piecewise linear segments. The series of $\delta_k(t)$ functions is computed for each value of t until the convergence criterion is met,

$$(23) \qquad |\delta_\eta(t) - \delta_{\eta-1}(t)| \leq e \quad , \qquad \eta = 0, 1, 2, \ldots$$

where e is a preset error. The approximation to f(t) is then

$$(24) \quad f(t) \simeq \frac{1}{\pi} \sum_{k=0}^{\eta} \left\{ \frac{f_k - f_{k+1}}{(\omega_{k+1} - \omega_k)} \left[1 - e^{i(\omega_{k+1} - \omega_k)t} \right] - \frac{f_k - f_{k+1}}{it} e^{i(\omega_{k+1} - \omega_k)t} \right\} e^{i\omega_k t}$$

for $t > 0$

Note that Eqn. (23) must be satisfied for each value of t so that η is not constant and must be computed for each value of t, or prescribed in the computation scheme in which case the convergence criterion Eqn. (23) is not necessarily met at each value of t.

NUMERICAL EXAMPLE OF INVERSE TRANSFORM

The function below

$$(25) \quad f(t) = \begin{cases} 0 & -\infty < t \leq -T \\ 1 - t/T & -T \leq t \leq 0 \\ 1 + t/T & 0 \leq t \leq T \\ 0 & T \leq t < \infty \end{cases}$$

the analytical Fourier integral transform of which is

$$(26) \quad \bar{f}(\omega) = T\left(\frac{\sin \omega T/2}{\omega T/2}\right)^2 \qquad \text{(Fig. 7).}$$

was used along with Eqn. (24) to generate an approximate inverse transform, or approximation to Eqn. (25) above for $t \geq 0$. The value of η was preset at 500 and the data points were equally spaced over the interval $0 \leq \omega \leq \frac{10\pi}{T}$,

or five zeros of the transform. The numerical results are shown in Table (1) for the case in which $T = 10^{-4}$ sec and $\eta = 500$. One observes that the approximate inverse transform $\overset{*}{f}(t)$ differs from f(t) (computed from Eqn. (25) above) in the third digit over the first 9/10 of the time interval, and in second digit over the last 1/10 of the time interval. In Table (2) the results are listed for $\eta = 1000$, $T = 10^{-4}$ for the same data point spacing, i.e. over ten zeros of the transform. An additional digit of accuracy was picked up for each of the time intervals, three digit accuracy for the first 9/10 of the time interval $0 \leq t \leq T$ and about two digit accuracy over the last 1/10 of the time interval.

In Table (3) are the results of nine cases in which inverse transforms of Eqn. (26) were computed using Eqn. (24) and using a finite difference approximation to Eqn. (17), or a discrete inverse transform. Both computed transforms were compared to the analytic value given by Eqn. (25). The relative error* range for each computed transform is shown in the fifth column of Table 3 for the piecewise linear approximation and in the sixth column for the discrete, or finite difference version. One can see that the piecewise linear method is more accurate than the discrete finite difference method for the same number (k) of data points of $\bar{f}(\omega)$ used in the computations and that the difference in accuracy becomes more pronounced as k decreases.

ANALYSIS OF WAVE PROPAGATION DATA

It is well known that a one dimensional wave propagating in a relaxing medium such as a linear viscoelastic polymeric material (eg. low density polyethylene[2]) or water containing a large concentration of air bubbles[1] obeys the wave equation having a complex phase velocity or

$$(27) \quad \frac{\partial^2 \psi(x,t)}{\partial x^2} = \frac{1}{\overset{*}{C}^2} \frac{\partial^2 \psi(x,t)}{\partial t^2} \quad .$$

The wave function $\psi(x,t)$ can be stress, strain, or particle velocity for a viscoelastic wave or pressure for a compression wave in a dispersive fluid. Taking the Fourier integral transform of Eqn. (27) we obtain, for zero initial conditions,

---

*relative error is analytic value minus computed value all divided by the analytic value.

$$(28) \qquad \frac{\partial^2 \bar{\psi}(x,\omega)}{\partial x^2} - \lambda^2(\omega)\bar{\psi}(x,\omega) = 0$$

in which $\bar{\psi}(x,\omega)$ is the Fourier transform of $\psi(x,t)$ and $\lambda(\omega)$ is the complex wave number defined by

$$(29) \qquad \lambda(\omega) = \alpha(\omega) + i\omega/C(\omega).$$

(Note: by virtue of Eqn. (27) that $\lambda^2 = -\omega^2/\overset{*}{C}{}^2$)

The solution to Eqn. (28) is

$$(30) \qquad \bar{\psi}(x,\omega) = Ae^{-\lambda x} + Be^{\lambda x}$$

in which A and B are constants to be determined from boundary conditions. If ψ is finite as x increases without bound then B must be zero. Assuming that the wave function at x = 0 is a known function $\psi(0,t)$, transforming and then substituting into Eqn. (30) yields $A = \bar{\psi}(0,\omega)$. Equation (30) becomes

$$(31) \qquad \bar{\psi}(x,\omega) = \bar{\psi}(0,\omega)e^{-\alpha x}e^{-i\omega x/C} = \bar{\psi}(0,\omega)\, e^{-\lambda x}.$$

If the wave function at some other spatial location is known, say $\psi(L,t)$, then α and C can be obtained from the transforms $\bar{\psi}(0,\omega)$ and $\bar{\psi}(L,\omega)$ by employing Eqn. (31). If we define

$$(32) \qquad G(\omega) = \bar{\psi}(L,\omega)/\bar{\psi}(0,\omega)$$

then Eqn. (31) yields

$$(33) \qquad \alpha(\omega) = -\frac{1}{2L}\, \ell n(|G(\omega)|)$$

and

$$(34) \qquad C(\omega) = \omega L/\cos^{-1}[\mathrm{Re}\{G(\omega)\}/|G(\omega)|]$$

After C and α are obtained, Eqn. (31) then is the source of the transform of the wave function at any coordinate x provided the material really does obey Eqn. (27). The wave function at any x coordinate $\psi(x,t)$ can then be obtained by inverting $\psi(x,\omega)$.

For convenience in data reduction the function $\psi(L,t)$ is translated to

the time origin by changing variables. Letting $t' = t - T_p$, where T_p is time of first arrival of any disturbance at $x = L$, it can be shown that

$$(35) \quad \bar{\psi}(L,\omega) = \overset{*}{\bar{\psi}}(L,\omega)e^{-i\omega T_p}$$

in which $\overset{*}{\bar{\psi}}(L,\omega)$ is the Fourier Transform of the time translated version of $\psi(L,t)$ or $\psi(L, t' + T_p)$. The formulae of α and C then become

$$(36) \quad \alpha(\omega) = -\frac{1}{2L} \ln(|\overset{*}{G}(\omega)|)$$

$$(37) \quad C(\omega) = C_o/[1 + \frac{1}{\omega T_p} \cos^{-1}(\mathrm{Re}\{\overset{*}{G}(\omega)\}/|\overset{*}{G}(\omega)|)]$$

where

$$(38) \quad \overset{*}{G}(\omega) = \overset{*}{\bar{\psi}}(L,\omega)/\psi(0,\omega)$$

and

$$(39) \quad C_o = L/T_p$$

NUMERICAL EXAMPLES

Recently Stevens and Malvern[2] and Norris[6] have published experimental data obtained from one dimensional viscoelastic wave propagation experiments with different types of polyethylene filaments. In each experimental program $\alpha(\omega)$ and $C(\omega)$ values were measured by means of sinusoidal steady-state vibration experiments. The results for each program can be seen in Figs. 10 and 11 for Stevens and Malvern and for Norris, respectively. In each case, a smooth curve was fitted to the α and C data and values derived from the curves were used to predict the wave function at another point by employing a finite-difference numerical inversion scheme to evaluate the inverse transforms. Norris used a measured stress-time function at $x = 0$ to predict particle velocity $V(x,t)$ at three locations by numerical evaluation of

$$(40) \quad V(x,t) = \frac{1}{\pi} \mathrm{Re}\left\{ \int_o^\infty \frac{\bar{\sigma}(0,\omega)}{\rho C(\omega)} \exp(-\alpha x) \exp[i\omega(t - x/C)]d\omega \right\}$$

Stevens and Malvern used a measured particle velocity-time curve at one station to predict the particle velocity at another by numerically integrating

$$(41)\quad V(x,t) = \frac{1}{\pi}\int_0^\infty \mathrm{Re}\,\{\bar{V}(0,\omega)\}\cos\,(\omega(t - x/C))$$

$$- \mathrm{Im}\,\{\bar{V}(0,\omega)\}\sin\,[\omega(t - x/C)]\,e^{-\alpha x}\,d\omega$$

where

$$(42)\quad \bar{V}(0,\omega) = \mathrm{Re}\{\bar{V}(0,\omega)\} + i\ \mathrm{Im}\{\bar{V}(0,\omega)\}$$

which was obtained exactly by means of a piecewise linear approximation of $V(0,t)$. Eqn. (41) was not evaluated exactly, however. Instead a finite difference numerical integration scheme was used.

Two numerical examples were chosen to demonstrate the numerical method of wave propagation data analysis. This author has taken the data at the first two stations of both Stevens' and Malvern's data and Norris' data and, using the previously-discussed technique of obtaining exact Fourier transforms of piecewise linear approximations to the data, obtained the values of $\alpha(\omega)$ and $C(\omega)$ numerically from the wave propagation data by means of Eqn. (35), (36) and (37). The data points on each set of curves, Fig. 12, 13, were connected by straight lines to form the piecewise linear functions approximating the smooth curves. The calculated values of $\alpha(\omega)$ and $C(\omega)$ and the Fourier transform of the data measured at the first station were substituted into Eqn. (31) to obtain the Fourier transform of the wave function at any downstream station. This transform was inverted numerically using Eqn. (24) to obtain the wave function (particle velocity) at a particular spatial location. The predicted numerical values are superposed on the measured curves in Fig. 12 and 13. For both sets, fairly good agreement with experimental results are obtained. In the case of Norris' data, slightly better agreement was achieved using this method than was achieved by Norris using another scheme.

COMPUTER PROGRAM

The computer program which calculates the numerical transforms at two locations, computes $\alpha(\omega)$ and $C(\omega)$, and predicts the wave at some downstream point is listed in the Appendix as Program 3. A complete listing, sample input and output data, and a detailed write-up is available from the Author on request.

CONCLUSIONS

A method of computing Fourier integral transforms of continuous data by approximating the data with piecewise linear segments, the exact Fourier transforms of which are known, leads to a more accurate method of approximating the Fourier transform of the continuous data by means of a series of exact transforms, rather than by finite difference numerical integration methods, or discrete transforms.

This method of computing Fourier transforms has been applied to the analysis of viscoelastic wave propagation data and the material properties of the viscoelastic medium calculated. In addition, the method of computing inverse transforms has been applied successfully in the prediction of wave motion along a viscoelastic bar and the results have been shown to compare favorably with existing published experimental data.

REFERENCES

1. Carstensen, E. L. & Foldy, L. L., "Propagation of Sound Through a Liquid Containing Bubbles," J.A.S.A., 19, (5), 401-501, (1947).

2. Stevens, A. L. and Malvern, L. G., "Wave Propagation in Prestrained Polyethylene Rod," Experimental Mechanics, Vol. 10, No. 1, January 1970, pp. 24-30.

3. Magrab, E. B. and Ochsner, D. J., "Transient Response of a Visco-elastic Bar Subjected to a Time-Dependent End - Displacement," SIAM J. Appl. Math., Vol. 16, No. 6, pp. 1266-1279, 1968.

4. G-AE Subcommittee on Measurement Concepts, "What is the Fast Fourier Transform?," IEEE Trans. on Audio and Electroacoustics, Vol. AU-15, No. 2, June 1967.

5. Cooley, J. W., Lewis, P. A. W., Welch, P. D., "The Finite Fourier Transform," IEEE Trans. on Audio and Electroacoustics, Vol. AU-17, No. 2, June 1969.

6. Norris, Douglas M. Jr., "Propagation of a Stress Pulse in a Visco-elastic Rod," Experimental Mechanics, Vol. 7, No. 7, pp. 297-301, 1967.

TABLE 2

TIME t (sec)	ANALYTIC VALUE f(t)	COMPUTED VALUE $\hat{f}(t)$	ERROR DIFFERENCE $\lvert f(t) - \hat{f}(t) \rvert$
.000000	.100000+01	.989869	.202310-02
.100000-04	.900000-00	.899590-00	.410080-03
.200000-04	.800000-00	.799876-00	.124410-03
.300000-04	.700000-00	.699931-00	.693500-04
.400000-04	.600000-00	.599945-00	.548288-04
.500000-04	.500000-00	.499950-00	.500455-04
.600000-04	.400000-00	.399955-00	.449158-04
.700000-04	.300000-00	.299970-00	.304617-04
.800000-04	.200000-00	.200011-00	.106115-04
.900000-04	.100000+00	.100175+00	.174774-03
.990000-04	.100000-01	.109761-01	.976073-03

$\eta = 1000$, $T = 10^{-4}$ sec

TABLE 3

RUN NO.	NUMBER DATA POINTS(k)	FREQUENCY INCREMENT (cps)	PIECEWISE LINEAR TRANSFORM RELATIVE ERROR RANGE	DISCRETE INTEGRATION RELATIVE ERROR RANGE
1	1000	100	$.1 \times 10^{-4} \rightarrow .9 \times 10^{-1}$	$.2 \times 10^{-3} \rightarrow .1 \times 10^{1}$
2	1000	400	$.4 \times 10^{-4} \rightarrow .4 \times 10^{-1}$	$.3 \times 10^{-3} \rightarrow .5 \times 10^{1}$
3	500	100	$.3 \times 10^{-3} \rightarrow .5 \times 10^{0}$	$.1 \times 10^{-2} \rightarrow .19 \times 10^{1}$
4	500	1000	$.1 \times 10^{-4} \rightarrow .4 \times 10^{-1}$	$.2 \times 10^{-3} \rightarrow .1 \times 10^{2}$
5	500	2000	$.4 \times 10^{-4} \rightarrow .12 \times 10^{0}$	$.1 \times 10^{-3} \rightarrow .2 \times 10^{2}$
6	100	100	$.1 \times 10^{-1} \rightarrow .4 \times 10^{1}$	$.1 \times 10^{-1} \rightarrow .5 \times 10^{1}$
7	100	1000	$.1 \times 10^{-3} \rightarrow .9 \times 10^{-1}$	$.1 \times 10^{-2} \rightarrow .1 \times 10^{2}$
8	50	2000	$.1 \times 10^{-2} \rightarrow .3 \times 10^{-1}$	$.4 \times 10^{-2} \rightarrow .2 \times 10^{2}$
9	25	4000	$.2 \times 10^{-2} \rightarrow .3 \times 10^{0}$	$.8 \times 10^{-2} \rightarrow .4 \times 10^{2}$

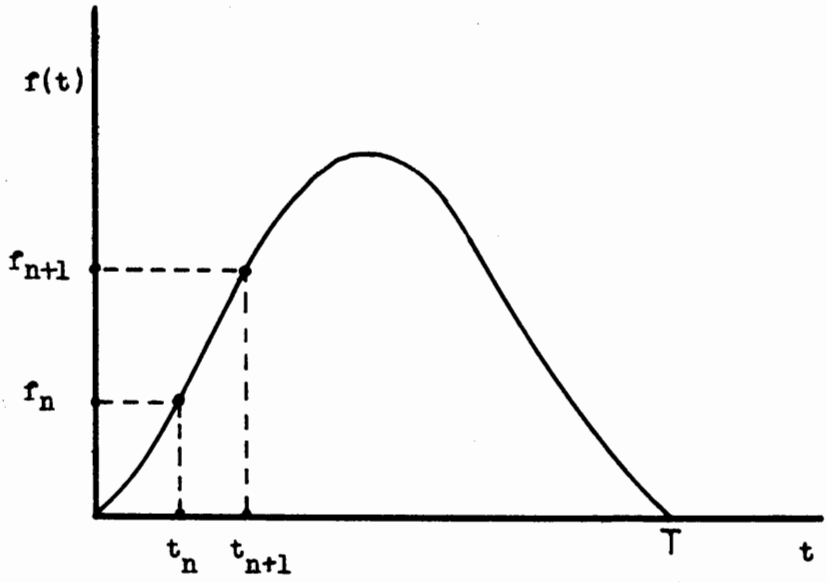

Figure 1. Typical analog pulse data to be transformed. Region between t_n and t_{n+1} to be approximated by straight line.

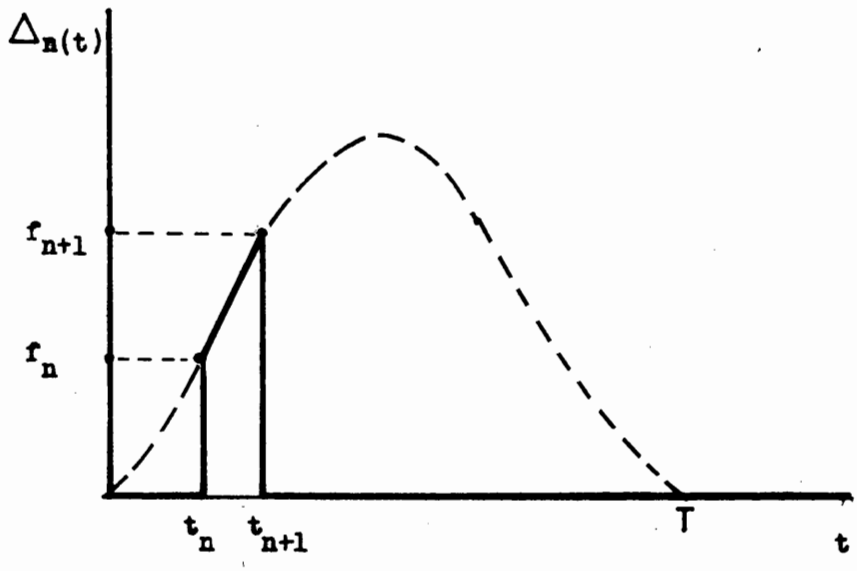

Figure 2. Approximating "alias" function for f(t) between t_n and t_{n+1}.

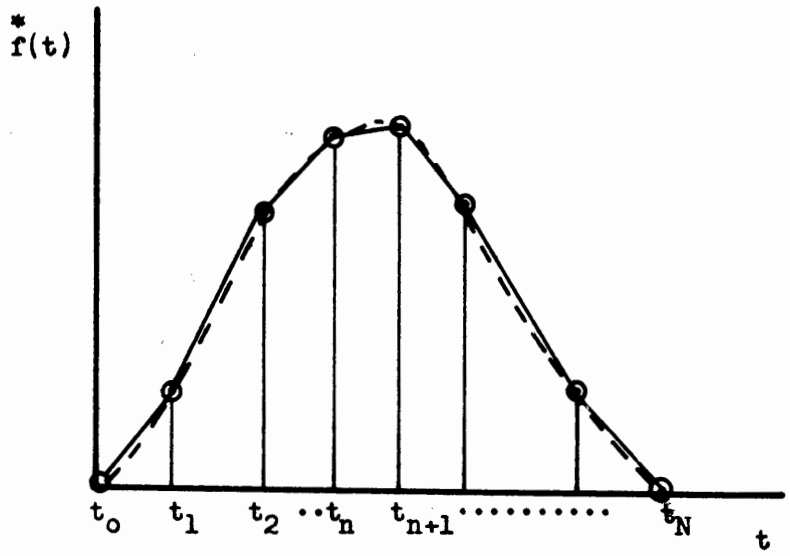

Figure 3. Piecewise linear approximating ("alias") function replacing f(t) before taking transform. Analytic transform of "alias" function is known.

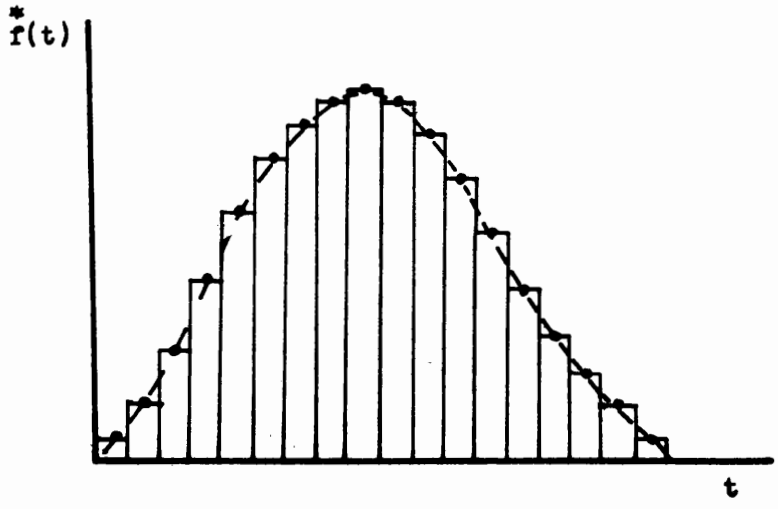

Figure 4. Approximating function comprised of rectangular pulses. Transform of this "alias" function is related to a discrete transform in Eqn. (15).

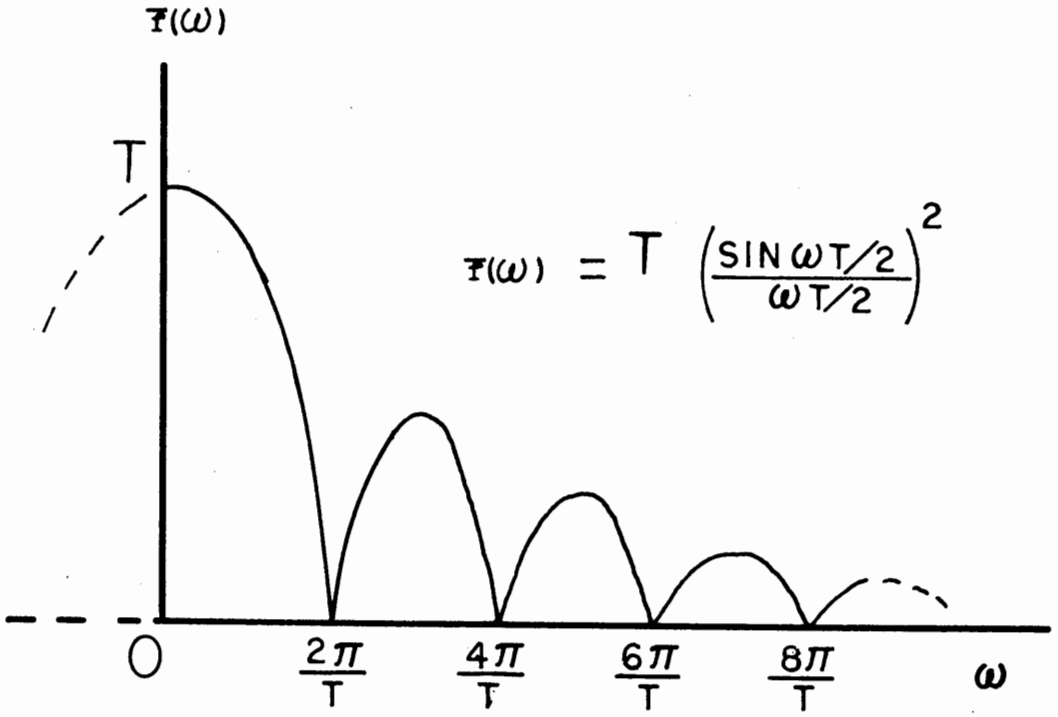

Figure 7. Analytic Fourier integral transform of function described in Fig. 6. Transform is symmetric about the ordinate axis. Numerical inverse Fourier integral transforms are obtained for this function.

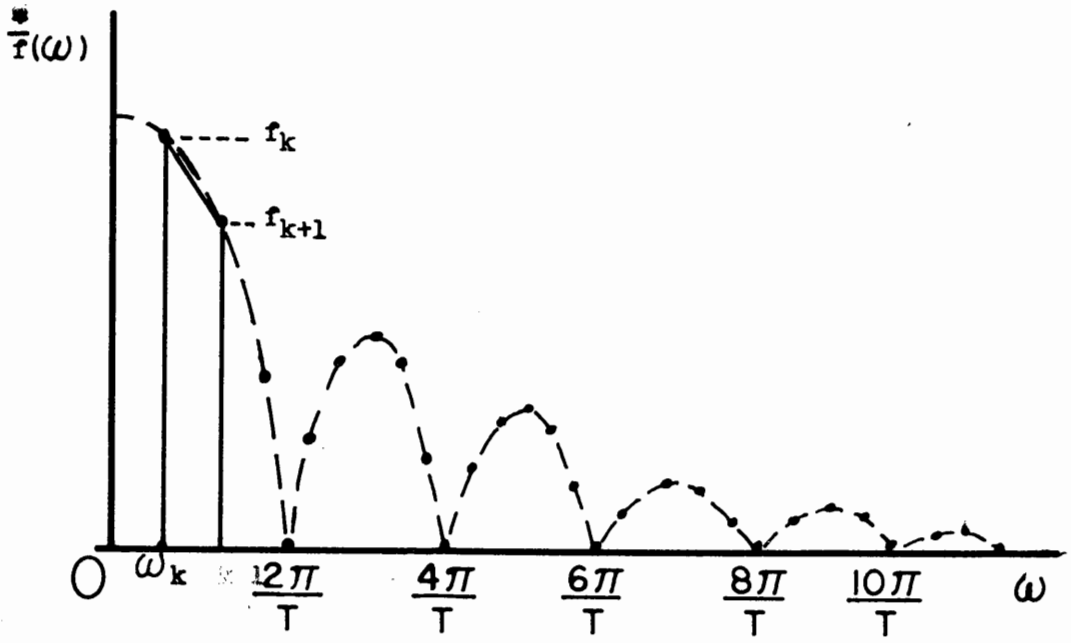

Figure 8. Linear "alias" function approximating the transform function is shown connecting data points f_k and f_{k+1}.

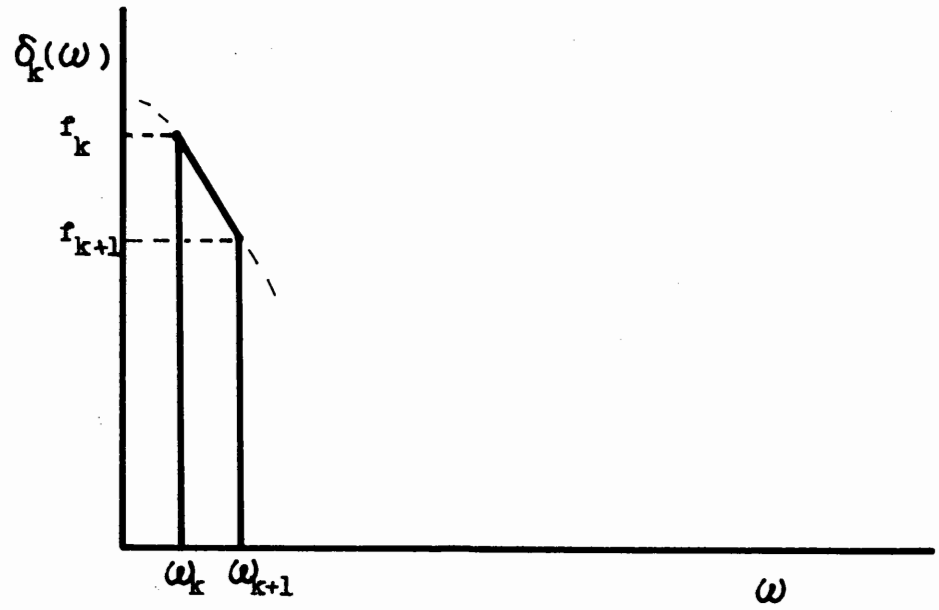

Figure 9. Linear approximating function. Function is zero outside interval $\omega_k \leq \omega \leq \omega_{k+1}$.

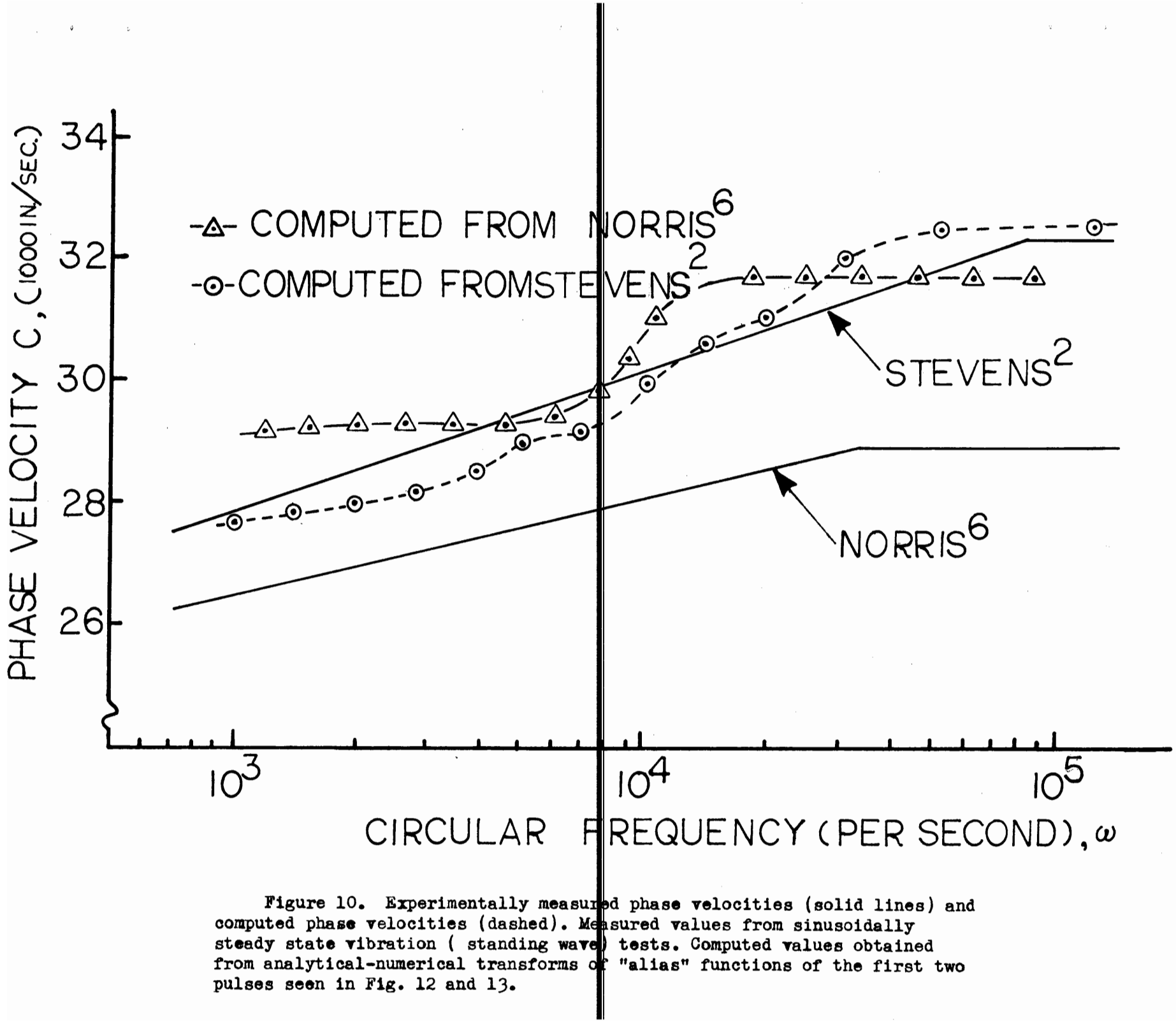

Figure 10. Experimentally measured phase velocities (solid lines) and computed phase velocities (dashed). Measured values from sinusoidally steady state vibration (standing wave) tests. Computed values obtained from analytical-numerical transforms of "alias" functions of the first two pulses seen in Fig. 12 and 13.

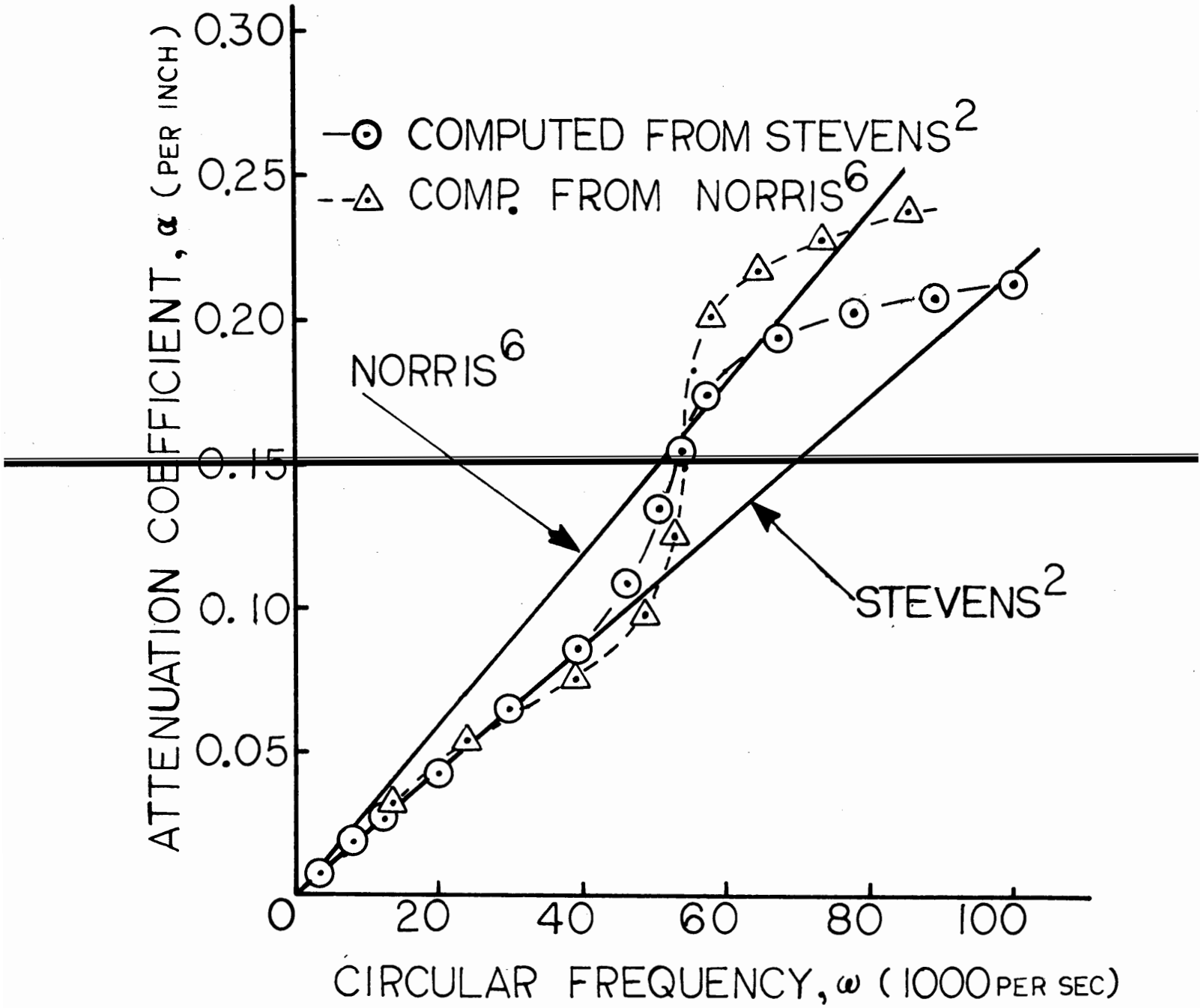

Figure 11. Experimentally measured attenuation coefficients (solid curves) and computed attenuation coefficients (dashed curves). Measured values obtained from sinusoidally steady state vibration (standing wave) tests. Computed values obtained from analytical-numerical transforms of "alias" functions of the first two pulses seen in Fig. 12 and 13.

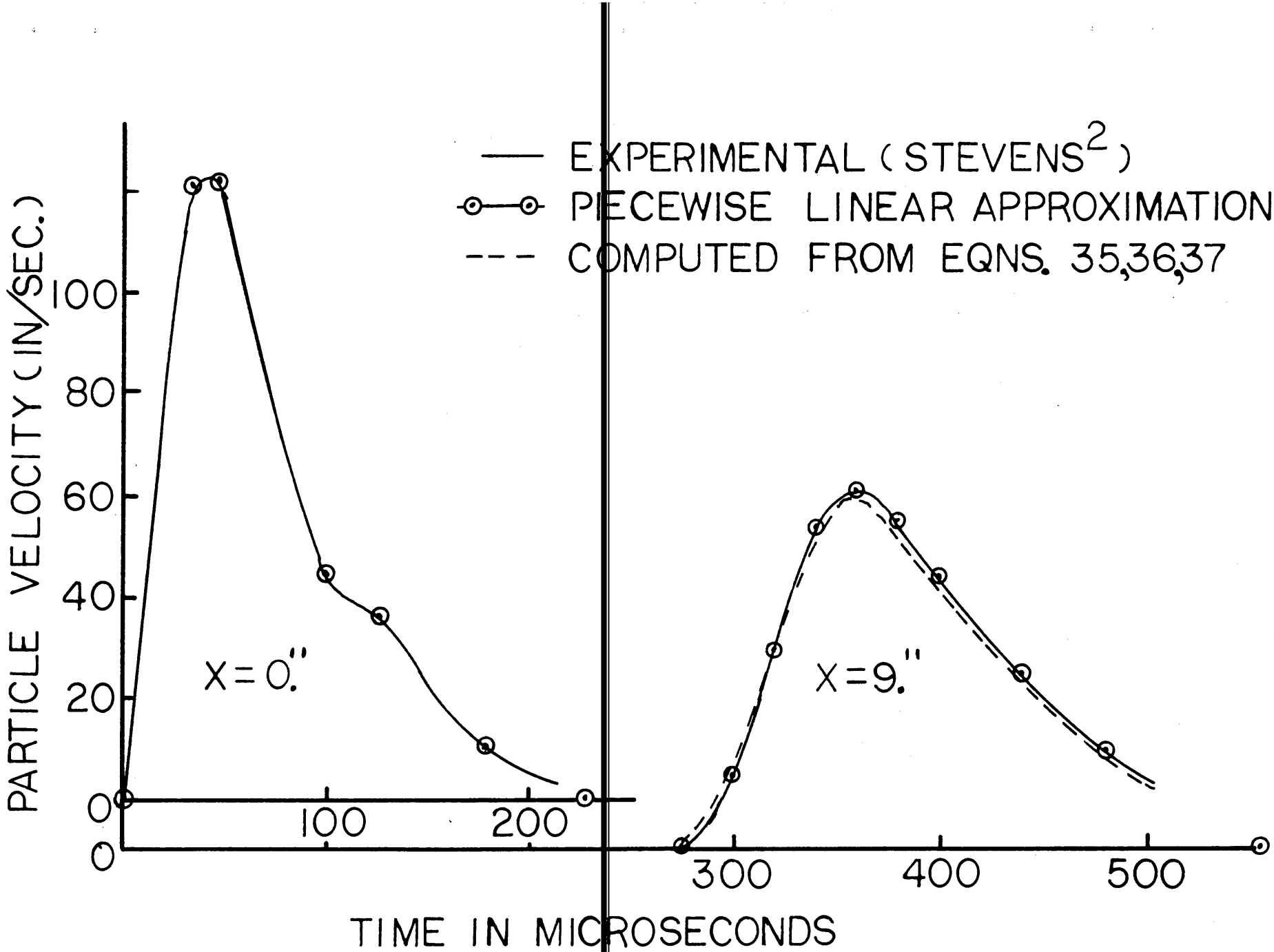

Figure 12. Comparison of experimental viscoelastic wave propagation data with predicted pulse using the analytical-numerical transform method. Phase velocities and attenuation coefficients were computed from alias functions describing the two pulses and used to predict the second pulse. Close agreement of computed pulse to measured pulse indicates accuracy of the method.

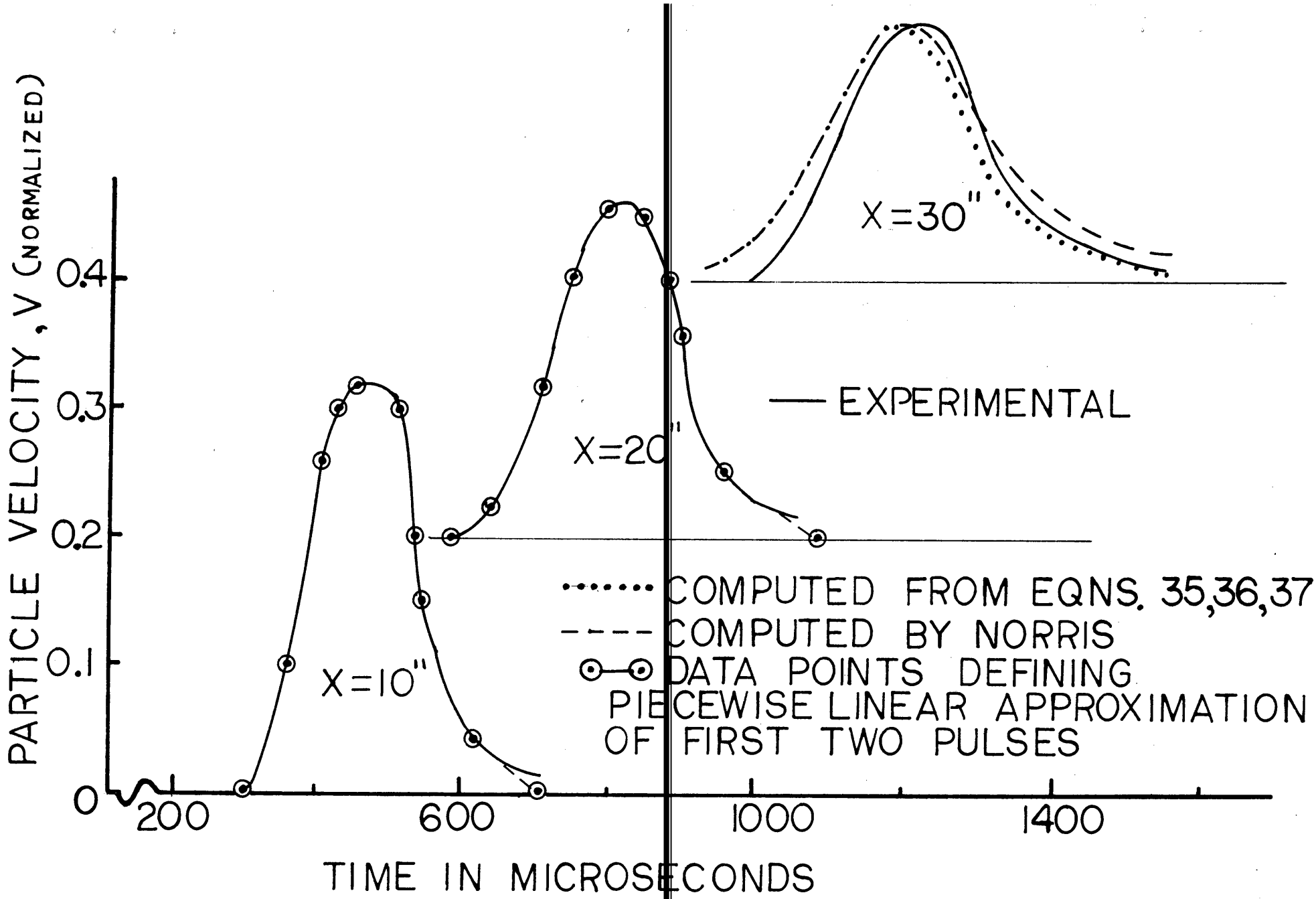

Figure 13. Comparison of experimental viscoelastic wave propagation data with predicted pulse using the analytical-numerical transform method. Phase velocities and attenuation coefficients were computed from "alias" functions describing the first two pulses and used , along with the approximate Fourier transform of the first pulse to predict the third pulse. Predicted pulse is seen to agree with experimental values and values predicted by Norris, using a different set of numerical initial values and a different finite-difference numerical integration scheme.

APPENDIX

PROGRAM I

Fourier Transform

The first computer program listed below permits computation of the Fourier Transform of the function given in Eqn. (25) for $T = 10^{-4}$ sec and compare the results to values of the analytic transform given in Eqn. (26) and to values of the discrete transform computed from Eqn. (3), over the range of frequency $0 \leq f \leq 10^5$ ps in increments of $\Delta f = 10^3$ cps. Output columns, 2, 4, and 6 are the numerical values of the analytical numerical method, discrete finite difference transform, and the known analytic value, respectively. As the columns indicate, the analytical-numerical values agree with the analytic values to the fifth or sixth digit while the finite-difference discrete method yield values which agree with the analytic result only to the third digit. As Eqn. (15) suggests, the error of the discrete method increases with frequency.

Running time on Univac 1108 was 43 sec.

FOURIER TRANSFORM

```
      DIMENSION TRANM(1000),TRANO(1000),FREQ(1000),TRANC(1000)
     1DIF2(1000),DIF1(1000)
      COMPLEX TRANM,TRANO,AJ,BJ
      COMMON TR
C     READ INPUT DATA
      READ 80, NSETS
80    FORMAT(14)
      DO 51 J=1,NSETS
      READ 80, K, NH
      READ 81, ERR
81    FORMAT (F8.4)
      READ 82, TR, TL
82    FORMAT (2E10.3)
      N=NH/(2*ERR)
      DELTAT=(TR-TL)/N
      DELTAF=NH/(K*(TR-TL))
      PI=3.14159265
      DO 50 KK=1, K
      IF(KK-1)11,10,11
10    DO 54 NN=1,N
      TIME2=   NN*DELTAT+TL
      TIME1=TIME2-DELTAT
      AFC=(FCN(TIME1)+FCN(TIME2))/2
54    TRANM(KK)=TRANM(KK)+AFC*DELTAT
11    AJ=(0,1.)
      BJ=AJ*(-1)
      DO 20 NN=1, N
      TIME2=   NN*DELTAT+TL
      TIME1=TIME2-DELTAT
      W=2*PI*(KK-1)*DELTAF
      T1=TIME1
      T2=TIME2
      DT=DELTAT
      IF(KK-1)61,62,61
61    TRANM(KK)=TRANM(KK)+((FCN(T1)-FCN(T2))/(W**2*DT)*(1-CEXP(BJ*W*DT))
     1+(FCN(T1)-FCN(T2)*CEXP(BJ*W*DT))/(AJ*W))*CEXP(BJ*W*T1)
62    TRANO(KK)=TRANO(KK)+(FCN(TIME2)+FCN(TIME1))/2.*CEXP((-1)*AJ*
     1(KK-1)*DELTAF*2*PI*TIME1)*DELTAT
20    CONTINUE
      IF(KK-1)14,13,14
13    TRANC(KK)=TR
      GOTO 15
14    TRANC(KK)=TR*((SIN(PI*TR*(KK-1)*DELTAF))/(PI*TR*(KK-1)*DELTAF))**2
15    DIF1(KK)=1-TRANM(KK)/TRANC(KK)
      DIF2(KK)=1-TRANO(KK)/TRANC(KK)
50    FREQ(KK)=(KK-1)*DELTAF
      PRINT 80, NSETS, K, NH, N
      PRINT 82, ERR, DELTAT, DELTAF
      PRINT 84, (FREQ(I),TRANM(I),TRANO(I),TRANC(I),DIF1(I), DIF2(I)
     1,I=1,K)
84    FORMAT(1HO,8(4X,E13.6))
51    CONTINUE
      END
```

OUTPUT PROGRAM I

1	2	3	4	5	6	7	8
.100000+04	.967530-04	-.251857-09	.967529-04	.121584-06	.967531-04	.135601-05	.23692
.150000+05	.450316-05	-.181143-11	.450210-05	.848721-07	.450316-05	.208616-06	.23688
.250000+05	.162114-05	-.422063-12	.162007-05	.509131-07	.162114-05	.163913-06	.65816
.350000+05	.827112-06	.585095-12	.826045-06	.363552-07	.827112-06	-.894070-07	.12895
.450000+05	.500352-06	-.687702-12	.499286-06	.282634-07	.500352-06	-.105798-05	.21304
.550000+05	.334946-06	.482588-12	.333880-06	.231133-07	.334946-06	-.387430-06	.31827
.650000+05	.239813-06	-.754828-12	.238747-06	.195446-07	.239813-06	.210106-05	.44457
.750000+05	.180126-06	-.577278-12	.179060-06	.169256-07	.180127-06	.460446-05	.59199
.850000+05	.140237-06	.229812-11	.139172-06	.149246-07	.140237-06	-.326335-05	.75959
.950000+05	.112268-06	-.134778-11	.111203-06	.133375-07	.112267-06	-.233948-05	.94835

PROGRAM II

Inverse Fourier Transform

The second computer program listed below permits computation of the inverse Fourier transform of the function given in Eqn. (26) for $T = 10^{-4}$ sec and compares the result to the known analytic inverse transform given by Eqn. (25) for $t \geq 0$. Two outputs of the program are listed in Tables (1) and (2). Running time on Univac 1108 was 48 seconds.

INVERSE FOURIER TRANSFORM

```
      DIMENSION F(1000),TIM(1000),INT(1000),ER(1000)
      REAL INT
      COMPLEX AJ
      PI=3.14159265
      T=1,0E-04
      AJ=(0.,1.)
      DF=1,0E+02
      N=100
      K-1000
      DW=2*PI*DF
      DT=1,0E-06
      DO 1 I=1,K
      W=(I-1)*DW
      F1=(I-1)*DF
      F2=I*DF
      IF(I,EQ,1) GO TO 2
      F1BAR=((SIN(PI*T*F1))**2)/((PI*F1*T)**2) *T
      GO TO 4
2     F1BAR=1  *T
4     F2BAR=((SIN(PI*T*F2))**2)/((PI*F2*T)**2) *T
      DO 3 NN=2,N
      TIM(NN)=(NN-1)*DT
3       INT(NN)=INT(NN)+1/PI*((F1BAR-F2BAR)/(DW*TIM(NN)**2)*(1-CEXP(
     1AJ*DW*TIM(NN)))-(F1BAR-F2BAR*CEXP(AJ*DW*TIM(NN)))/(AJ*TIM(NN)))
     2*CEXP(AJ*W*TIM(NN))
      INT(1)=INT(1)+(F1BAR+F2BAR)/  DF
1     CONTINUE
      DO 5 NN=1,N
      F(NN)=1-(NN-1)*DT/T
      ER(NN)=F(NN)-INT(NN)
5     PRINT 6 TIM(NN),F(NN),INT(NN),ER(NN)
6     FORMAT (4(10X,E13,6))
      END
```

PROGRAM 3

PROGRAM VISCOWAVE

```
      DIMENSION T1(1000), F1(1000),TR1(2000),T2(1000),F2(1000),TR2(2000)
     1,ALFA(2000),C(2000)
      COMMON T1,T2
      DOUBLE PRECISION C
      COMPLEX TR1, TR2
      COMMON/TWO/NH,K,NP,TMAX,TIM2
      READ 99,NSETS
99    FORMAT(I5)
      DO 100 II=1,NSETS
      READ 1,N,K,NH,M,NP,ERR,EX,TMAX,EX3,TIM3,TIM2
1     FORMAT(5I5,5E10.3,/,E10.3)
      PI=3.14159265
      PRINT1,N,K,NH,M,NP,ERR,EX,TMAX,EX3,TIM3,TIM2
      READ 2(T1(I),I=1,N)
      READ 2(F1(I),I=1,N)
2     FORMAT(7E10.3)
      READ 2(T2(I),I=1,M)
      READ 2(F2(I),I=1,M)
      READ 3,HSHIF1,VSHIF1,HSCAL1,VSCAL1
      READ 3,HSHIF2,VSHIF2,HSCAL2,VSCAL2
3     FORMAT(4E10.3)
      DO 4 I=1,N
      T1(I)=(T1(I)-HSHIF1)*HSCAL1
4     F1(I)=(F1(I)-VSHIF1)*VSCAL1
      DO 5 I=1,M
      T2(I)=(T2(I)-HSHIF2)*HSCAL2
5     F2(I)=(F2(I)-VSHIF2)*VSCAL2
      PRINT 32(T1(I),F1(I),T2(I),F2(I),I=1,M)
32    FORMAT(4(6X,E13.6))
      CALL TRAN(T1,F1,N,ERR,TR1,KP)
      CALL TRAN(T2,F2,M,ERR,TR2,KQ)
      CALL MATPRO(TR1,TR2,EX,KP,KQ,ALFA,C,KR)
100   CALL PREDIK(ALFA,C,TR1,EX3,TIM3,KR)
      END
```

```
      SUBROUTINE TRAN(T,F,N,ERR,TR,KP)
      DIMENSION T(1000),F(1000),TR(2000),FREQ(2000)
      COMPLEX TR,AJ,BJ
      COMMON/ONE/PI
      COMMON/TWO/NH,K,NP,TMAX,TIM2
      IB=0
      PI=3.14159265
    1 DELTAF=NH/(K*TMAX)
      DELTAW=DELTAF*2*PI
      DO 84 KK=1,K
   84 TR(KK)=(0.,0.)
      NC=0
      KN = N-1
      DO 50 KK=1,K
      IF(KK-1)11,10,11
   10 DO 54 NN=1,KN
      DT=T(NN+1)-T(NN)
   54 TR(KK)=TR(KK)+(F(NN)+F(NN+1))/2*DT
   11 AJ=(0.,1.)
      BJ=(-1)*AJ
      DO 20 NN=1,KN
      DT=T(NN+1)-T(NN)
      W=(KK-1)*DELTAW
      IF(KK-1)61,20,61
   61 TR(KK)=TR(KK)+((F(NN)-F(NN+1))/(W**2*DT)*(1-CEXP(BJ*W*DT)) +
     1(F(NN)-F(NN+1)*CEXP(BJ*W*DT))/(AJ*W))*CEXP(BJ*W*T(NN))
   20 CONTINUE
      FREQ(KK)=(KK-1)*DELTAF
   50 CONTINUE
      PRINT 99(FREQ(KK),TR(KK)      ,KK=1,K)
   99 FORMAT(3(6X,E13,6))
      KP=K
      RETURN
      END
```

```
      SUBROUTINE  MATPRO(TR1,TR2,EX,KP,KQ,ALFA,C,KR)
      DIMENSION TR1(2000),TR2(2000),ALFA(2000),C(2000)
     1,FREQ(2000),CC(7)
     3,T1(1000),T2(1000)
      COMMON T1,T2
      DOUBLE PRECISION C,ARG,D,E
      COMPLEX TR1,TR2,GW
      COMMON/TWO/NH,K,NP,TMAX,TIM2
      COMMON/ONE/PI
      KR=MINO(KP,KQ)
      C(1)=EX/TIM2
      DO 1 KK=2,KR
      FREQ(KK)=(KK-1)*NH/(K*TMAX)
      W=2*PI*FREQ(KK)
      GW=TR1(KK)/TR2(KK)
      D=REAL(GW)
      E=AIMAG(GW)
      ALFA(KK)=0, 5/EX*DLOG(D**2+E**2)
      DO 3 IP=1,7
      IPP=IP-4
      ARG=D/(SQRT(D**2+E**2))
    3 CC(IP)=C(1)/(1+C(1)/(W*EX)*( -DACOS(ARG)+2*IPP*PI))
       C(KK)=C(1)/(1+C(1)/(W*EX)*(  DACOS(ARG)))
    9 PRINT2,FREQ(KK),C(KK),ALFA(KK),(CC(IP),IP=1,6),ARG
    2 FORMAT(1X,E11,4,1X,D11,4,7(1X,E11,4),1X,D11,4)
    1 CONTINUE
      RETURN
      END
```

```
      SUBROUTINE  PREDIK(ALFA,C,TR1,EX3,TIM3,KR)
      DIMENSION ALFA(2000),C(2000),          TR3(2000),F(1000),T(1000)
     1,TR1(2000),LAMDA(1000), S(1000)
      DOUBLE PRECISION C
      COMPLEX TR1,TR3,LAMDA,AJ,F
      COMMON/ONE/PI
      COMMON/TWO/NH,K,NP,TMAX,TIM2
      DELTAF=NH/(K*TMAX)
      AJ=(0.,1.)
      DELTAW=2*PI*DELTAF
      KR=KR-1
      DO 2 NN=1,NP
      T(NN)=(NN-1)*TMAX/(NP-1)+TIM3
      S(NN)=T(NN)-EX3/C(KK)
      DO 2 KK=1,KR
      W=(KK-1)*DELTAW
      CW=C(KK)
      LAMDA(KK)=ALFA(KK)+AJ*W/CW
      CWD=C(KK+1)
      LAMDA(KK+1)=ALFA(KK+1)+AJ*(W+DELTAW)/CWD
      TR3(KK+1)=TR1(KK+1)*CEXP(-LAMDA(KK+1)*EX3)
      TR3(KK)=TR1(KK)*CEXP(-LAMDA(KK)*EX3)
    2 F(NN)=F(NN)+1/PI*((TR3(KK)-TR3(KK+1))/(DELTAW*T(NN)**2)*(1-CEXP(AJ
     1*DELTAW*T(NN)))-(TR3(KK)-TR3(KK+1)*CEXP(AJ*DELTAW*T(NN)))/
     2(AJ*T(NN)))*CEXP(AJ*W*T(NN))
      PRINT 9,(T(NN),F(NN),NN=1,NP)
    9 FORMAT(3(10X,E13.6))
    3 FORMAT(2(10X,E13.6))
      RETURN
      END
```

UNCLASSIFIED

Security Classification

DOCUMENT CONTROL DATA - R & D

Security classification of title, body of abstract and indexing annotation must be entered when the overall report is classified)

1. ORIGINATING ACTIVITY (Corporate author)	2a. REPORT SECURITY CLASSIFICATION
SOUTHERN METHODIST UNIVERSITY	UNCLASSIFIED
	2b. GROUP UNCLASSIFIED

3. REPORT TITLE

An approximate Fourier integral transform method for analysis of wave propagation signals

4. DESCRIPTIVE NOTES (Type of report and inclusive dates)

Technical Report

5. AUTHOR(S) (First name, middle initial, last name)

Hal Watson, Jr.

6. REPORT DATE	7a. TOTAL NO. OF PAGES	7b. NO. OF REFS
July 13, 1970	38	6

8a. CONTRACT OR GRANT NO.	9a. ORIGINATOR'S REPORT NUMBER(S)
N00014-68-A-0515	
b. PROJECT NO. NR 042-260	73
c.	9b. OTHER REPORT NO(S) (Any other numbers that may be assigned this report)
d.	

10. DISTRIBUTION STATEMENT

This document has been approved for public release and sale; its distribution is unlimited. Reproduction in whole or in part is permitted for any purpose of the United States Government.

11. SUPPLEMENTARY NOTES	12. SPONSORING MILITARY ACTIVITY
	Office of Naval Research

13. ABSTRACT

Analysis of sound wave signals often requires obtaining Fourier integral transforms of short duration pulses. The transforms are usually difficult to obtain analytically because of the lack of a precise analytical description of the pulses. Therefore, the Fourier integrals are usually obtained numerically by using a time series to approximate the pulse and by approximating the integral with a finite series, thereby approximating the Fourier integral with a finite difference numerical integration scheme. In this paper an analytical numerical scheme of computing approximate Fourier integral transforms is discussed. The scheme allows the analytical description of the transform of a piecewise linear "alias" function which approximates the original pulse. The analytical description is in the form of a finite series the number of terms of which is equal to the number of linear segments comprising the alias function. The series is then available for algorithmic computation on an automatic digital computer. This scheme is shown to be more accurate than the finite numerical integration scheme.

Ths analytical-numerical transform scheme is used to analyze sound wave pulses in a viscoelastic, dispersive medium and the results are compared with known experimental data.